energies

MDPI

Article

Chemical Characteristics and NaCl Component Behavior of Biochar Derived from the Salty Food Waste by Water Flushing

Ye-Eun Lee [1,2], Jun-Ho Jo [1], I-Tae Kim [1] and Yeong-Seok Yoo [1,2,*]

[1] Division of Environment and Plant Engineering, Korea Institute of Civil Engineering and Building Technology 283, Goyang-daero, Ilsanseo-gu, Goyang-si, Gyeonggi-do 10223, Korea; yeeunlee@kict.re.kr (Y.-E.L.); junkr@kict.re.kr (J.-H.J.); itkim@kict.re.kr (I.-T.K.)

[2] Department of Construction Environment Engineering, University of Science and Technology, 217, Gajeong-ro, Yuseong-gu, Daejeon KS015, Korea

* Correspondence: ysyoo@kict.re.kr; Tel.: +82-31-910-0298; Fax: +82-31-910-0288

Received: 21 August 2017; Accepted: 30 September 2017; Published: 10 October 2017

Abstract: Biochar is the product of the pyrolysis of organic materials in a reduced state. In recent years, biochar has received attention due to its applicability to organic waste management, thereby leading to active research on biochar. However, there have been few studies using food waste. In particular, the most significant difference between food waste and other organic waste is the high salinity of food waste. Therefore, in this paper, we compare the chemical characteristics of biochar produced using food waste containing low- and high-concentration salt and biochar flushed with water to remove the concentrated salt. In addition, we clarify the salt component behavior of biochar. Peak analysis of XRD confirms that it is difficult to find salt crystals in flushed char since salt remains in the form of crystals when salty food waste is pyrolyzed washed away after water flushing. In addition, the Cl content significantly decreased to 1–2% after flushing, similar to that of Cl content in the standard, non-salted food waste char. On the other hand, a significant amount of Na was found in pyrolyzed char even after flushing resulting from a phenomenon in which salt is dissolved in water while flushing and Na ions are adsorbed. FT-IR analysis showed that salt in waste affects the binding of aromatic carbons to compounds in the pyrolysis process. The NMR spectroscopy demonstrated that the aromatic carbon content, which indicates the stability of biochar, is not influenced by the salt content and increases with increasing pyrolysis temperature.

Keywords: salty food waste; FT-IR; pyrolysis; biochar; NaCl

1. Introduction

The process of dealing with food waste affects climate change by emitting large amounts of greenhouse gases such as methane and carbon dioxide [1]. The Food and Agriculture Organization has reported that one-third of the produced food in the world is thrown away annually [2]. As a result, a new alternative is needed to deal with the vast amounts of food waste.

Biochar is the product that results from the pyrolysis of organic materials in a reduced state. It is distinguished from charcoal by its usage as a soil amendment [3]. Biochar can be produced from a variety of materials including wood, agricultural waste, and livestock waste [4]. Biochar also reduces the release of organic carbon into the air in the form of carbon dioxide by resisting microbial degradation [5,6]. It also helps to prevent climate change by reducing the emission of greenhouse gases such as nitrogen oxides from the soil and methane [7]. Mitchell et al. [8] studied the characteristics of biochar from pyrolyzed lignocellulosic municipal waste, and Prakongkep et al. [9] compared and analyzed 14 types of tropical plant-waste-derived biochar. In addition, Kwapinski et al. [10]

analyzed the temperature-related characteristics of biochar generated from pyrolyzing miscanthus, pine, and willow as a waste management method. They analyzed the characteristics of biochar as a soil amendment and fertilizer. Most studies on biochar have used wood or vegetable raw materials; few have used salty food wastes as raw materials.

As the applicability of biochar to organic waste management has received attention, various studies have been done on its chemical [11] and physical characteristics [12], and its effect on soil [13]. The major difference between other organic materials and biochar is the large proportion of aromatic carbon [14]. Secondly, biochar consists mostly of immobile carbon and nitrogen that microorganisms cannot use as energy sources, thereby having chemical stability (ASTM standard methodology) [15]. In addition, the difference involves cation exchange capacity (CEC) of biochar resulting from the surface charge. Pyrolysis condition is an important factor in determining the physicochemical characteristics of biochar [16]. Hossain et al. [17] revealed that the composition and chemical structure of biochar changed according to the pyrolysis temperature by pyrolyzing the sewage sludge at 300–700 °C. Cantrell et al. [18] showed that the source type could alter the physicochemical characteristics by pyrolyzing five types of manure at 350 and 700 °C.

The major difference between municipal waste (organic waste), such as sewage sludge, livestock waste, and agricultural by-products, and food waste is its high salinity [19,20]. The high salt content of food waste is a major obstacle to recycling and treating food waste. Therefore, we investigate the effect of salt on the conversion into biochar by analyzing the characteristics of pyrolyzed char according to salt content. In this paper, the chemical characteristics of biochar produced using food waste containing low- and high-concentration salt and biochar flushed with water to remove the concentrated salt are compared and analyzed. In addition, the salt component behavior of biochar is clarified.

2. Experimental

2.1. Raw Material

The food waste samples were prepared as shown in Table 1 according to the composition of the standard sample, which is the average food waste composition ratio as determined by the Ministry of Environment of Korea [21]. Food wastes were classified into grains, vegetables, fruits, and meat and fish, and the composition ratios were set to 16%, 51%, 14%, and 19%, respectively, using 10 kinds of materials. The food samples were dried at 80 °C for 48 h and then ground into powder form. NaCl solution was added such that the NaCl contents relative to the dry weight of the food samples became 1%, 3%, and 5%. The samples were then dried again.

Table 1. The standard food waste sample.

Classification	Composition Ratio (wt %)	Methods of Food Ingredient Processing	
		Food Ingredients	Processing Method
Grains	16	Rice (16)	
Vegetables	51	Napa cabbage (9)	Cutting width less than 100 mm.
		Potato (20) Onion (20) Daikon (2)	Chop into 5 mm size pieces.
Fruits	14	Apple (7) Mandarin/Orange (7)	Split into 8 pieces in lengthwise.
Meat and Fish	19	Meat (4)	Cutting width around 3 cm.
		Fish (12)	Split into 4 pieces.
		Egg shell (3)	
Total	100	100	

2.2. Experimental Methods

Dry food samples containing 1%, 3%, and 5% NaCl were pyrolyzed in a pyrolysis reactor of 300 °C, 400 °C, and 500 °C. They were pyrolyzed for 1 h and 30 min, and 10 L/min nitrogen gas was continuously injected. Figure 1 shows the schematic diagram of the pyrolysis apparatus used in this experiment, which consisted of a nitrogen inlet, specimen vat, sample chamber, furnace, a cooling device, and gas combustion device. The total dimensions of pyrolysis reactor are 150 cm * 180 cm * 50 cm and the cooler temperature is maintained at 10 °C. The specimen vat size is 4.5 cm * 5 cm * 20 cm (H * W * D) and only two specimen vat put in the reactor. Feed weight is 100 g each specimen vat. Nitrogen gas was injected 10 min before the samples were added to prevent oxidation of the samples. The temperature in the furnace increased to the target temperature of 300 °C, 400 °C, and 500 °C, and the samples in the sample chamber were then added. The mass yield of biochar at each temperature is 0.56, 0.38, and 0.32 as the pyrolysis temperature increases 300 to 500 °C, and the biochar yields are decreased as the pyrolysis temperature increases [22].

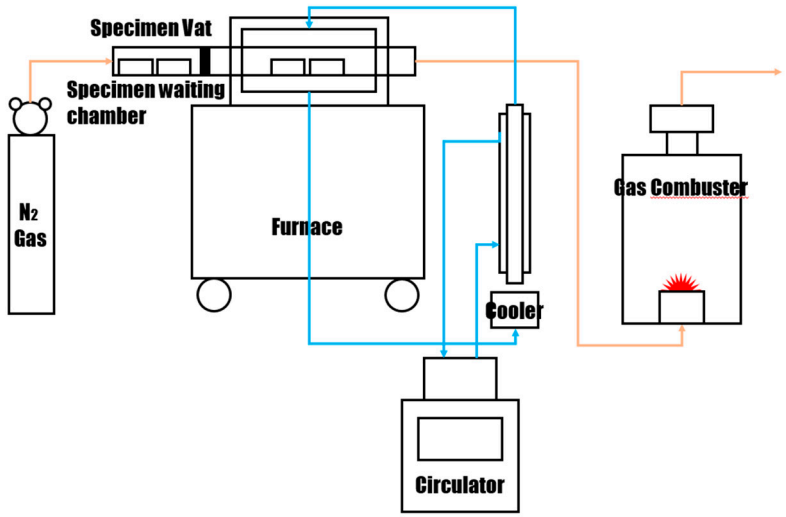

Figure 1. The schematic diagram of the pyrolysis apparatus.

After pyrolysis, the samples were removed, cooled to room temperature, weighed, and ground. They were flushed by stirring 30 g of char in 300 mL of distilled water at a ratio of 1:10 for 30 min. The flushed char was then separated using a filter paper and dried again at 80 °C for 24 h before being stored.

2.3. Analytical Methods

2.3.1. Characterization

A FLASH EA1112 instrument (Thermo Electron, Waltham, MA, USA) was used for the elementary analysis (C, H, S, N) of the salty food waste derived biochar. Oxygen is obtained by difference assuming the sum of C, H, S, N, O, Ash, and NaCl is 100%. In general, either Na or Cl is measured to determine the salt content. However, one study reported a phenomenon in which Na and Cl are independently volatilized in the pyrolysis process of saline-containing fossil fuel [23]. Therefore, both the Na and Cl contents were measured independently. Na content was measured using Agilent 5100 ICP-OES (Agilent Technologies, Santa Clara, CA, USA). Cl was carbonized after mixing 2.5–5 g samples with the milk of lime and drying. 1–2 drops of potassium chromate were added to the sample, which was filtrated after adding water and shaking. The solution was titrated with silver nitrate solution [24]. To measure Cation exchange capacity (CEC) values, 5 g of the sample was then placed in a 100 mL Erlenmeyer flask, and 50 mL of 1 M NH_4OA_c solution was added [25]. The sample was

then shaken for 30 min, filtered, and diluted. The CEC was measured using Agilent 5100 ICP-OES (Agilent Technologies). The Na, K, Mg, and Ca contents were calculated by converting the measured absorbance value (ppm) using the Brown's simplified method.

2.3.2. X-ray Diffraction Spectroscopy

X-ray diffraction (XRD) analysis was carried out to determine the structure of salt in the salty food waste derived-biochar and the change in the molecular structure both before and after flushing. The analytical equipment used was DMAX 2500 (Rigaku, Tokyo, Japan), and the X-ray generator had specifications of 18 kW and 60 kV/300 mA. The 2θ range of the recorded sample was 10–90°.

2.3.3. FT-IR

The infrared spectroscopic analysis was conducted to investigate the effect of salt in salty food waste on the biochars during pyrolysis and its effect on flushing. A VERTEX 80V (Bruker Optics, Ettlingen, Germany) device was used, and infrared rays of 400–4000 nm wavelength were transmitted to determine the characteristics. A transmission analysis was conducted using KBr powder.

2.3.4. NMR

The structure was analyzed using solid-state magic angle spinning ^{13}C NMR analysis to confirm the formation of aromatic carbons, which indicate the stability of the biochar. A DIGITAL AVANCE III 400 MHz (Bruker Biospin AG, Fällanden, Switzerland) was used with a 4 mm probe.

3. Results and Discussion

3.1. Chemical Composition of Salty Food-Waste-Derived Biochar

Table 2 shows the elementary analysis of the salty food waste derived biochar and Na and Cl contents. After flushing, the Cl content decreased to the Cl content in the STD sample, non-salted food waste sample. On the other hand, the Na content significantly increased after flushing compared to the Na content in the STD sample, non-salted food waste sample.

Table 2. The chemical compositions and atomic ratios of biochar produced by salty food waste.

Sample ID	Component, wt %							Atomic Ratio		
	C	H	N	O	Na	Cl	Ash	C/N	H/C	O/C
Dry	51.46	13.22	3.14	32.18	-	-	-	16.38	0.257	0.63
300 °C_STD	60.97	5.37	5.28	23.66	1.21	1.56	4.72	11.55	0.088	0.39
300 °C_1%_B	60.18	5.32	5.29	25.88	3.08	3.17	3.33	11.38	0.088	0.43
300 °C_1%_A	61.70	5.59	5.24	25.19	2.02	1.51	2.28	11.77	0.091	0.41
300 °C_3%_B	58.96	5.17	5.09	22.53	6.63	6.26	8.25	11.58	0.088	0.38
300 °C_3%_A	63.21	5.46	5.16	24.34	2.67	1.50	1.83	12.25	0.086	0.39
300°C_5%_B	57.29	5.04	4.98	20.83	9.30	8.74	11.86	11.5	0.088	0.36
300 °C_5%_A	62.08	5.81	5.42	23.03	2.62	1.50	3.66	11.45	0.094	0.37
400 °C_STD	64.69	3.64	5.09	17.82	1.92	1.90	8.76	12.71	0.056	0.28
400 °C_1%_B	63.27	3.60	5.38	17.98	4.74	4.18	9.77	11.76	0.057	0.28
400 °C_1%_A	68.71	4.28	5.04	17.60	4.01	1.20	4.37	13.63	0.062	0.26
400 °C_3%_B	57.85	3.24	4.16	21.08	9.22	8.25	13.67	13.91	0.056	0.36
400 °C_3%_A	65.43	3.70	5.26	20.94	3.43	1.19	4.67	12.44	0.057	0.32
400 °C_5%_B	56.15	3.20	3.99	18.74	16.53	12.66	17.92	14.07	0.057	0.33
400 °C_5%_A	68.43	4.34	4.51	19.47	4.64	1.36	3.25	15.17	0.063	0.28
500 °C_STD	70.11	2.81	5.23	8.83	0.51	0.90	13.02	13.41	0.04	0.13
500 °C_1%_B	68.82	2.71	5.22	10.45	3.98	3.74	12.80	13.18	0.039	0.15
500 °C_1%_A	72.07	2.93	5.13	9.43	3.43	1.03	10.44	14.05	0.041	0.13
500 °C_3%_B	65.72	2.69	4.63	10.33	9.65	9.42	16.63	14.19	0.041	0.16
500 °C_3%_A	72.10	2.98	5.13	11.32	5.14	1.49	8.47	14.05	0.041	0.16
500 °C_5%_B	61.78	2.43	4.44	10.50	15.56	13.80	20.85	13.91	0.039	0.17
500 °C_5%_A	73.28	2.92	4.92	11.80	5.35	1.45	7.08	14.89	0.04	0.16

Carbon content increased with the pyrolysis temperature, and there was a difference in the content before and after flushing that resulted from a slight increase in the carbon content relative to the total weight since salt was discharged while flushing.

Hydrogen content decreased as the pyrolysis temperature increased, and there was a difference in the content before and after flushing that resulted from increased relative weight since salt was discharged while flushing, as with carbon.

Nitrogen content did not show any tendency to increase or decrease according to the pyrolysis temperature. However, the nitrogen content of the biochar having 1% salt content decreased after flushing, while the nitrogen contents of the chars having 3% and 5% salt content increased after flushing.

The higher the pyrolysis temperature and the higher the salt content, the lower the O/C ratio, which indicates the stability of biochar [26]. There was a difference before and after flushing, but this phenomenon may have been caused by changes in salt content before and after flushing. When the O/C ratio is 0.2 or less, the half-life of biochar is estimated to be 1000 years or more. When the O/C ratio is 0.2–0.6, the half-life is estimated to be 100–1000 years [27]. The H/C ratio decreased as the pyrolysis temperature increased. There was an obvious difference according to pyrolysis temperature, but there was no difference according to the salt content. The Lower values of H/C and O/C at higher pyrolysis temperatures indicate a stable biochar with a low content of O-based functional groups by demethylation and decarboxylation [28].

A C/N ratio of 12:1 is the most favored for increasing the nitrogen pool plants can use, and a C/N ratio of 20:1 is used for soil conditioners, fertilizers and compost [29]. As the pyrolysis temperature increases, the C/N ratio increases [30]. The experimental result showed that the ratio increased and the ratio was 11–15, which is suitable for use in the soil when the temperature increased from 300 to 500 °C.

H/C, O/C, and C/N values are influenced by pyrolysis temperature, and the content of salt appears to have no noticeable effect on the chemical composition.

The CEC of salty food waste biochars varies depending on raw materials and pyrolysis conditions. Some studies have reported that the CEC value increases as the pyrolysis temperature increase from 300 to 500 °C in relation to the carboxyl groups on the biochar surface [31–33]. Table 3 shows that as the pyrolysis temperature increased from 300 to 400 °C, the CEC value increased, peaked at 400 °C, and decreased again at 500 °C. CEC is determined by substitution sites, O-based functional groups such as –OH or –COOH that are made by decarboxylation and deformation as the pyrolysis temperature. Although, further study is needed to specify the required energy for deformation to contain high CEC, it is reliable trend similar to Wu et al.'s study result [32]. These results may relate to specific surface area. Focusing on O-based functional groups, 300 °C should indicate highest CEC value. But in case of this, complex action between functional group and specific surface area, may be acted on the explanation of this phenomenon. O-based functional groups are decreased gradually as the pyrolysis temperature increases. Specific surface area is increased as the pyrolysis temperature increases [34]. At 300 °C, there could be more O based functional groups but there is lower specific surface area. Overall, the surface area of pyrolyzed char at 300 °C, including O-based functional groups, may be smaller than at 400 °C. About this assumption, further study is needed.

Table 3. CEC of salty food waste derived-biochar before and after flushing.

Sample ID	CEC (cmol/kg)	Extractable Cations (cmolc/kg)			
		Ca	K	Mg	Na
300 °C_STD	25.57	0.39	12.68	0.34	5.56
300 °C_1%_B	22.20	0.29	7.77	0.12	6.99
300 °C_1%_A	18.14	0.45	4.95	0.15	4.67
300 °C_3%_B	22.42	0.17	4.06	0.06	11.08
300 °C_3%_A	20.35	0.47	3.99	0.16	8.04
300 °C_5%_B	110.71	0.35	16.59	0.24	86.26
300 °C_5%_A	22.67	0.58	3.89	0.22	10.07
400 °C_STD	62.94	1.10	44.07	1.37	14.21
400 °C_1%_B	120.39	1.19	62.59	1.15	49.98
400 °C_1%_A	36.65	0.90	18.00	0.64	12.71
400 °C_3%_B	163.48	0.96	52.17	1.23	108.91
400 °C_3%_A	52.60	1.30	16.17	1.00	24.68
400 °C_5%_B	250.72	0.65	53.19	1.29	185.03
400 °C_5%_A	39.46	1.06	9.90	0.86	22.80
500 °C_STD	54.91	0.89	60.38	1.58	1.07
500 °C_1%_B	75.22	0.83	62.37	1.10	14.88
500 °C_1%_A	24.79	1.07	18.23	0.68	7.67
500 °C_3%_B	156.81	0.76	67.59	1.22	92.30
500 °C_3%_A	18.90	1.29	10.63	1.00	9.27
500 °C_5%_B	262.08	0.63	73.55	1.31	189.90
500 °C_5%_A	24.86	1.34	10.29	1.07	14.58

STD: Standard food waste biochar sample without NaCl. A: Salty food waste derived biochar after flushing. B: Salty food waste derived biochar before flushing.

Compared to the CEC value of the char unaffected by salt, the measured CEC value was higher before flushing and lower after flushing. This may have been the result of the phenomenon in which ionized Na^+ is adsorbed on the biochar surface during the flushing. VAN ZWIETEN et al. [35] showed that the application of biochar in a ferrosol significantly increased CEC of soil. In other words, the pyrolyzed salty food waste biochar is able to hold many cations which are nutritional content used by plants and helps the soil fertility improvement.

The extractable values of Na and K were much higher than those of other elements and significantly decreased after flushing. However, the extractable value of Ca increased after flushing. The value of Mg also increased in the case of 1% and 3% at 300 °C. This phenomenon will be discussed in relation to the result of Fourier transform infrared spectroscopy (FT-IR).

The CEC of soil is an important criterion for determining the ability of plants to retain the cations they use. Sandy soil, with its low organic content, has a CEC value of less than 3 cmolc/kg, but heavy clay soil or soil with a high organic content has a CEC value higher than 20 cmolc/kg [36]. Every sample except post-flushing samples (300 °C, 1%; 500 °C, 3%) obtained values higher than 20 cmolc/kg; therefore, it is expected that they are able to be used as soil conditioners.

3.2. XRD Analysis of Salty Food-Waste-Derived Biochar

Figures 2–5 show the XRD results of salty food waste chars before and after flushing according to the pyrolysis temperature, as well as those of NaCl. The crystalline form of NaCl has peaked at 32°, 45.5°, 56.5°, 66°, 75°, and 84° (2θ). When comparing these peaks with the XRD peaks of the salty food waste biochar, the graph before flushing clearly shows the NaCl peaks. On the other hand, the graph after flushing shows that the peaks of NaCl become blurred, and the peaks show a similar tendency to the peaks of standard food waste biochars containing no salt.

In other words, even after carbonization, NaCl remains in the form of crystals. However, after flushing, the remaining NaCl has washed away, and the peaks resemble those of the standard state.

The peak near 23° (2θ) corresponds to the diffuse graphite [37,38]. As the pyrolysis temperature increases, the peak shifts from 20° to 25° (2θ). This means that cellulose crystallinity decreases and turbostratic crystallinity increases [39].

As the pyrolysis temperature increases from 300 °C to 500 °C, the peak intensity near 28° (2θ) increases. This peak confirms the presence of calcite [40], and the sharper the peak, the better the calcite crystallization.

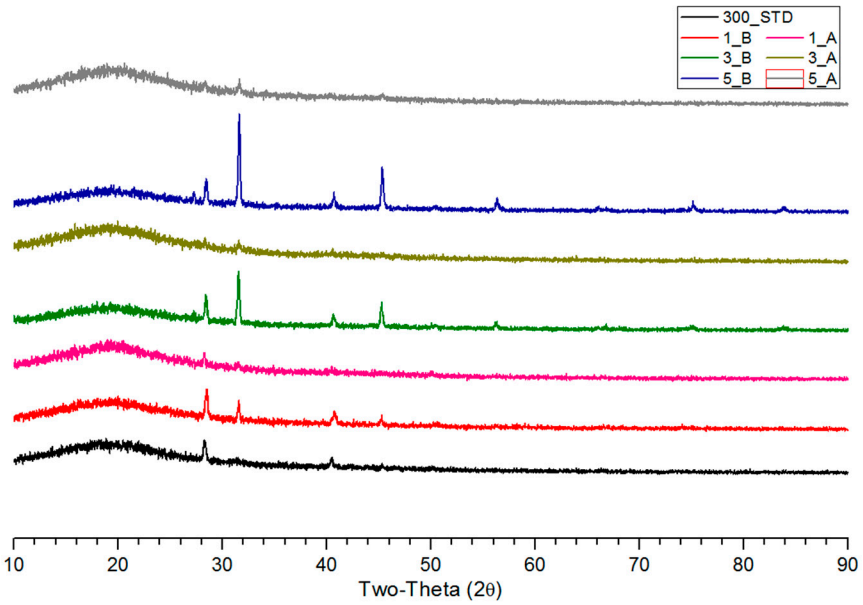

Figure 2. The XRD result of biochar pyrolyzed at 300 °C before and after flushing.

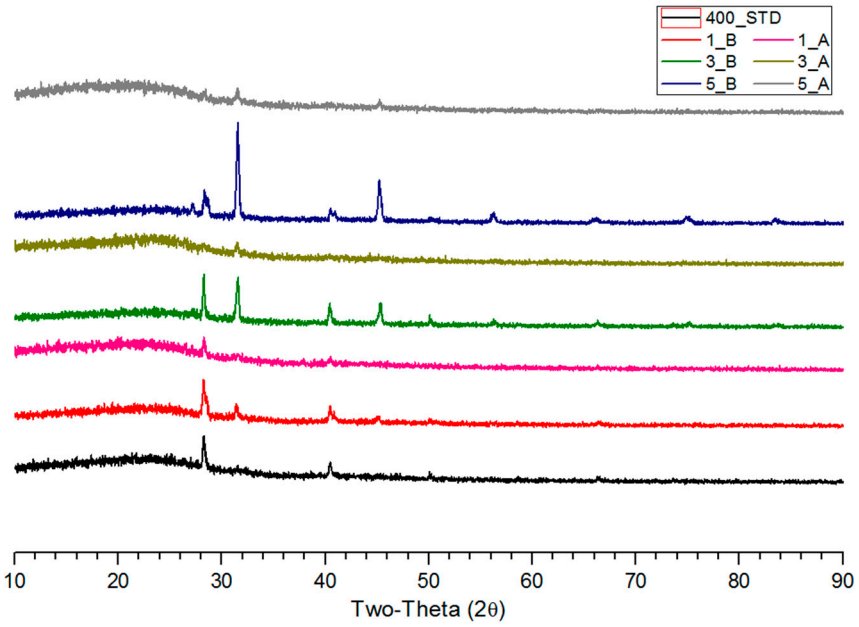

Figure 3. The XRD result of biochar pyrolyzed at 400 °C before and after flushing.

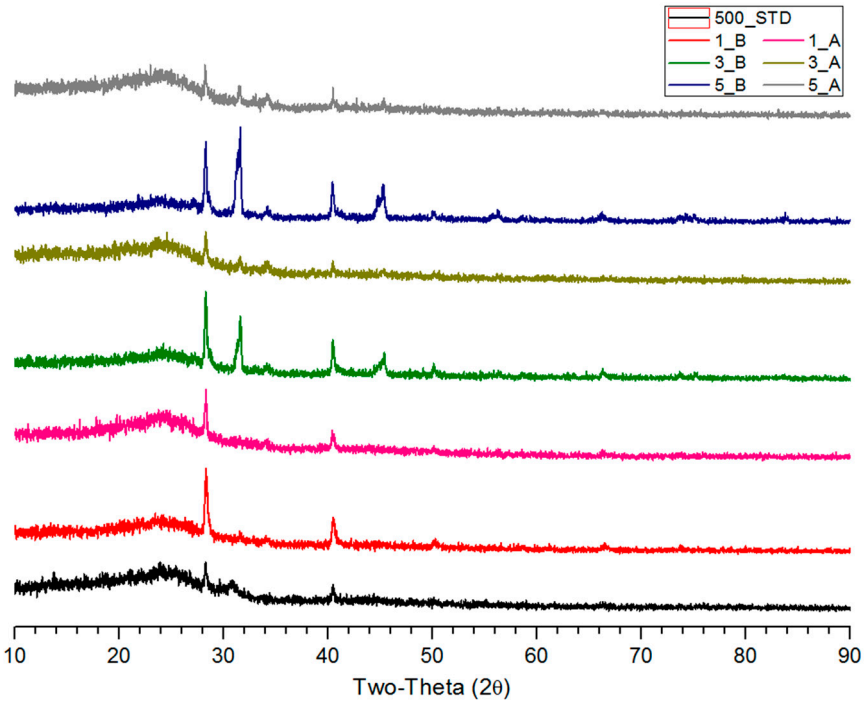

Figure 4. The XRD result of biochar pyrolyzed at 500 °C before and after flushing.

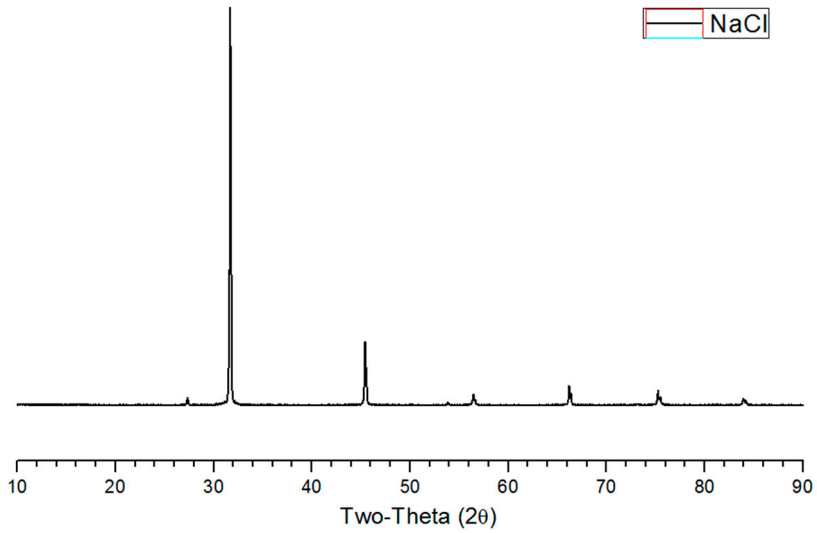

Figure 5. The XRD result of NaCl.

3.3. FT-IR Analysis of Salty Food-Waste-Derived Biochar

Figures 6–8, which show the FT-IR results for salty food waste biochars before and after flushing according to pyrolysis temperature, illustrate that the tendency varies significantly depending on the pyrolysis temperature.

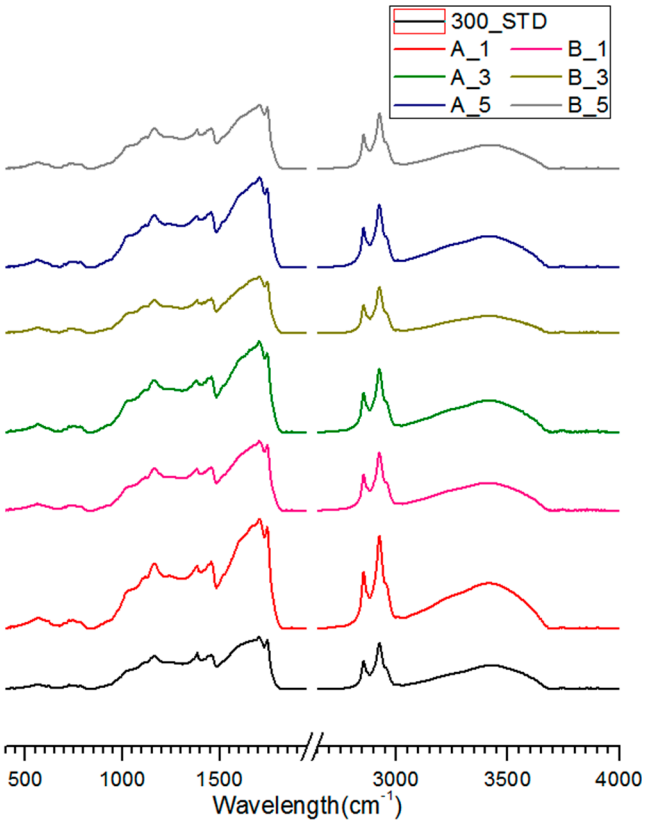

Figure 6. The FT-IR result of biochar pyrolyzed at 300 °C before and after flushing.

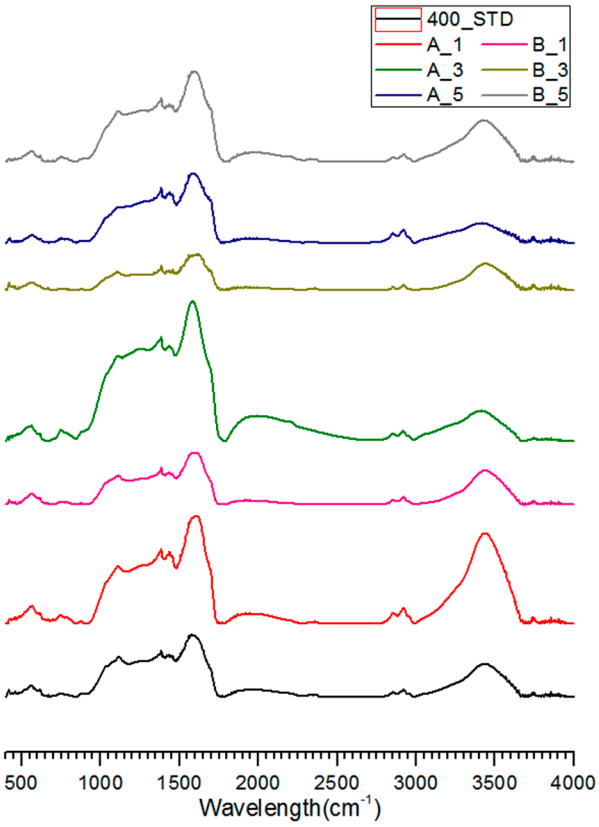

Figure 7. The FT-IR result of biochar pyrolyzed at 400 °C before and after flushing.

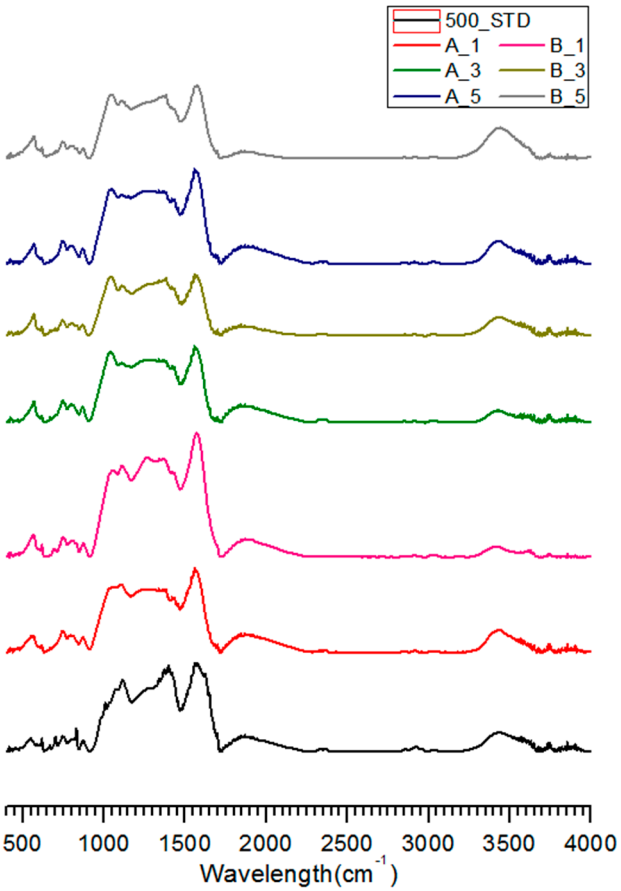

Figure 8. The FT-IR result of biochar pyrolyzed at 500 °C before and after flushing.

Carboxylic (COOH) bonds have a peak of 1700 cm^{-1} and are associated with CEC capability [41,42]. The peak near 1700 cm^{-1} that appeared clearly at 300 °C and 400 °C had almost disappeared at 500 °C. Decarboxylation occurred as the pyrolysis temperature increased, thereby decreasing the CEC value.

The peak near 1420–1440 cm^{-1} increased after flushing. This peak indicates a carboxylate anion [43]. It seems that NaCl is ionized while flushing and Na ions bind to the carboxylate anion, thereby intensifying the peak. The CEC values of Na and K were lower after flushing because Na was already bound, decreasing the capacity to exchange monovalent cations.

The distinctive peak change at 2800–3000 cm^{-1} indicates a change in aliphatic C-H, and the peak at 3600–3200 cm^{-1} reveals O-H hydroxyl groups [41,44]. As the pyrolysis temperature increased, the peak of the aliphatic C-H that was clear at 300 °C sharply decreased. The intensity of the peak was insignificant at 500 °C. The peak intensity of hydroxyl groups also gradually weakened. According to the elemental analysis, this demethylation phenomenon may have caused the decreased C/H ratio as the pyrolysis temperature increased.

The peak of aromatic C-H at 700–900 cm^{-1} [32,39] and the aromatic skeletal vibration peak at 1515–1590 cm^{-1} [42,45] became clearly visible and increased in intensity as the temperature increased from 300 °C to 500 °C. This confirms that aromatization occurred as the pyrolysis temperature and stability of biochar increased.

There were differences between the standard peak without any salt and the peak of pyrolyzed carbide containing salt. The peak shift from 550 cm^{-1} to 570 cm^{-1} was clearly shown as the pyrolysis temperature increased and salt content was higher. The peak near 550–600 cm^{-1} indicates C=O deformation of aromatic ketone [46]. Porchelvi and Muthu [47] investigated that the 552 cm^{-1} peak

results from SO_2 bound to deformed aromatic ketone and found that the 560 cm^{-1} peak appears due to cyano bound to a deformed aromatic ketone. In other words, a higher salt content induces more bonding of a specific compound to the aromatic ketone deformed in the pyrolysis process. More research is necessary for compounds that show a peak at about 570 cm^{-1}. In addition, the peak at 700 cm^{-1} appears in the standard without salt, while the peak is weak or does not appear at all in the presence of salt. This peak indicates the rocking vibration and binding of CH_2 with asymmetric deformation of aromatic ketone [47]. When salt is present, this bond is not induced. Thus, the salt contained in the food wastes affects the aromatic carbon in various biochar structures during the pyrolysis process.

Additionally, the peak at 520 cm^{-1}, which indicates the bonding of C-Cl [47], is not shown regardless of the pyrolysis temperature and salt content. This result demonstrates that the NaCl does not affect the biochar structure in the discrete state as Na^+ and Cl^-.

3.4. NMR Analysis of Salty Food Waste Derived Biochar

Figures 9–11 show the solid-state ^{13}C-NMR spectra. Although there is an apparent difference in the spectra according to the pyrolysis temperature, the peak shift by and influence of salt are negligible.

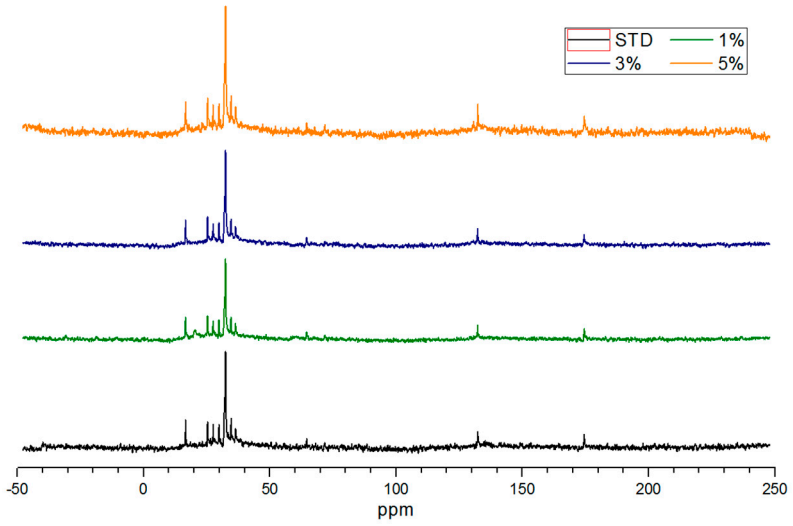

Figure 9. The NMR result of biochar pyrolyzed at 300 °C before and after flushing.

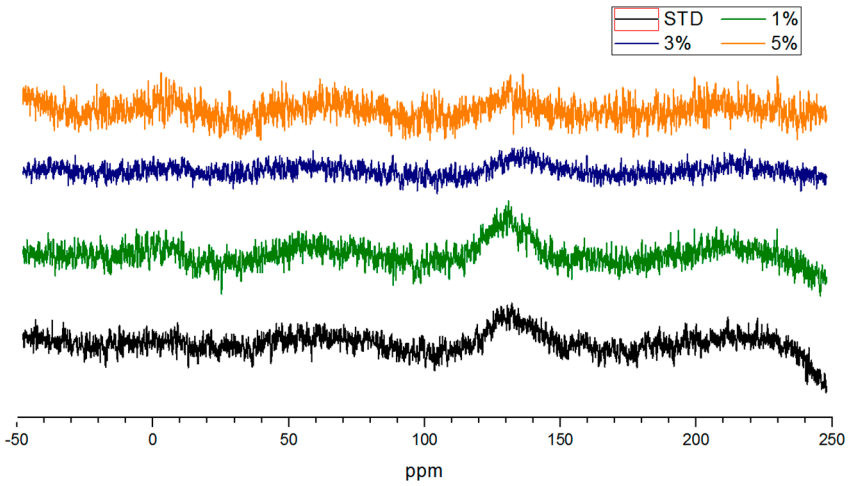

Figure 10. The NMR result of biochar pyrolyzed at 400 °C before and after flushing.

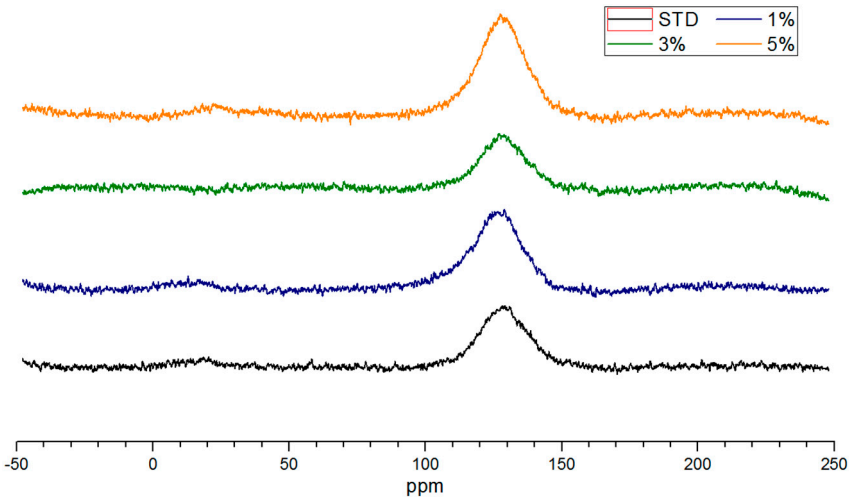

Figure 11. The NMR result of biochar pyrolyzed at 500 °C before and after flushing.

The peaks at 300 °C are shown at 16.5, 25–35, 64.5, 132, and 174.5 ppm, while broad peaks are seen from 128–132 ppm at 400 °C. At 500 °C, a weak peak is shown from 18–27 ppm and the distinct peak are seen from 110–150 ppm. The peak near 15 ppm represents CH_3 carbon, while the peak near 30–65 ppm indicates CH_2 carbon [48]. The aromatic C peak is shown narrowly around 130 ppm and also appears broadly in the range of 90–160 ppm [49,50]. The peak at 160–200 ppm means carboxylic or ketone C=O [41,50].

At 300 °C, significant amounts of CH_3 and CH_2 are present and form the main peak, while aromatic C is insufficient until demethylation occurs. As the pyrolysis temperature increases to 400 °C, sufficient dehydration occurs, and aromatic C is formed. At 500 °C, clearly visible aromatic C indicates the stabilized biochar.

4. Conclusions

In this paper, we analyzed the characteristics of pyrolyzed char according to salt content and temperature (300 °C to 500 °C) in order to determine the effect of salt on conversion into biochar. After flushing, NaCl that remains in crystalline form is washed away under all conditions, and some of Na ions that were washed off and ionized in water are adsorbed again. The pyrolysis temperature is a more important parameter than salt content for the biochar characteristics. As the charring temperature increases, salty food waste became a more stable biochar with lower H/C and O/C values and higher C/N values and aromatic carbon content. Salt content affects aromatic ketone bonding. The higher content of salt in food waste induces more bonding of a specific compound to the aromatic ketones formed in the pyrolysis process. Flushed salty food waste biochar could be recommended as a soil amendment, further studies are needed about the effect of aromatic ketone formation on the soil.

Acknowledgments: This study was supported by the major project (2017-0509) of the Korea Institute of Civil engineering and building Technology (KICT).

Author Contributions: Jun-Ho Jo and Yeong-Seok Yoo designed the experiment devices; Yeong-Seok Yoo and I-Tae Kim contributed to the analysis of experimental results; Ye-Eun Lee performed the experiments, analyzed the data, and wrote the paper.

Conflicts of Interest: The authors declare no conflict of interest.

References

1. Hall, K.D.; Guo, J.; Dore, M.; Chow, C.C. The progressive increase of food waste in America and its environmental impact. *PLoS ONE* **2009**, *4*, e7940. [CrossRef] [PubMed]

2. Venkat, K. The climate change and economic impacts of food waste in the United States. *Int. J. Food Syst. Dyn.* **2011**, *2*, 431–446.
3. Lehmann, J.; Joseph, S. Biochar for environmental management: An introduction. In *Biochar for Environmental Management: Science and Technology*; Lehmann, J., Joseph, S., Eds.; Earthscan: London, UK, 2009.
4. Ioannidou, O.; Zabaniotou, A. Agricultural residues as precursors for activated carbon production—A review. *Renew. Sustain. Energy Rev.* **2007**, *11*, 1966–2005. [CrossRef]
5. Lehmann, J. A handful of carbon. *Nature* **2007**, *447*, 143–144. [CrossRef] [PubMed]
6. Brassard, P.; Godbout, S.; Raghavan, V.G.S.; Palacios, J.H.; Grenier, M.; Zegan, D. The production of engineered biochars in a vertical auger pyrolysis reactor for carbon sequestration. *Energies* **2017**, *10*, 288. [CrossRef]
7. Taghizadeh-Toosi, A.; Clough, T.J.; Condron, L.M.; Sherlock, R.R.; Anderson, C.R.; Craigie, R.A. Biochar incorporation into pasture soil suppresses in situ nitrous oxide emissions from ruminant urine patches. *J. Environ. Qual.* **2011**, *40*, 468–476. [CrossRef] [PubMed]
8. Mitchell, P.J.; Dalley, T.S.L.; Helleur, R.J. Preliminary laboratory production and characterization of biochars from lignocellulosic municipal waste. *J. Anal. Appl. Pyrolysis* **2013**, *99*, 71–78. [CrossRef]
9. Prakongkep, N.; Gilkes, R.J.; Wiriyakitnateekul, W. Forms and solubility of plant nutrient elements in tropical plant waste biochars. *J. Plant Nutr. Soil Sci.* **2015**, *178*, 732–740. [CrossRef]
10. Kwapinski, W.; Byrne, C.M.P.; Kryachko, E.; Wolfram, P.; Adley, C.; Leahy, J.J.; Novotny, E.H.; Hayes, M.H.B. Biochar from biomass and waste. *Waste Biomass Valoriz.* **2010**, *1*, 177–189. [CrossRef]
11. Nguyen, B.T.; Lehmann, J.; Hockaday, W.C.; Joseph, S.; Masiello, C.A. Temperature sensitivity of black carbon decomposition and oxidation. *Environ. Sci. Technol.* **2010**, *44*, 3324–3331. [CrossRef] [PubMed]
12. Downie, A.; Alan, C.; Paul, M. Physical properties of biochar. In *Biochar for Environmental Management: Science and Technology*; Earthscan: London, UK, 2009.
13. Jin, H. Characterization of Microbial Life Colonizing Biochar and Biochar-Amended Soils. Ph.D. Thesis, Cornell University, Ithaca, NY, USA, 2010.
14. Lehmann, J.; Rillig, M.C.; Thies, J.; Masiello, C.A.; Hockaday, W.C.; Crowleye, D. Biochar effects on soil biota—A review. *Soil Biol. Biochem.* **2011**, *43*, 1812–1836. [CrossRef]
15. Deenik, J.L.; McClellan, T.; Uehara, G.; Antal, M.J.; Campbell, S. Charcoal volatile matter content influences plant growth and soil nitrogen transformations. *Soil Sci. Soc. Am. J.* **2010**, *74*, 1259–1270. [CrossRef]
16. Guizani, C.; Jeguirim, M.; Valin, S.; Limousy, L.; Salvador, S. Biomass Chars: The Effects of Pyrolysis Conditions on Their Morphology, Structure, Chemical Properties and Reactivity. *Energies* **2017**, *10*, 796. [CrossRef]
17. Hossain, M.K.; Strezov, V.; Chan, K.Y.; Ziolkowski, A.; Nelsona, P.F. Influence of pyrolysis temperature on production and nutrient properties of wastewater sludge biochar. *J. Environ. Manag.* **2011**, *92*, 223–228. [CrossRef] [PubMed]
18. Cantrell, K.B.; Hunt, P.G.; Uchimiya, M.; Novak, J.M.; Ro, K.S. Impact of pyrolysis temperature and manure source on physicochemical characteristics of biochar. *Bioresour. Technol.* **2012**, *107*, 419–428. [CrossRef] [PubMed]
19. Wang, X.; Selvam, A.; Chan, M.; Wong, J.W.C. Nitrogen conservation and acidity control during food wastes composting through struvite formation. *Bioresour. Technol.* **2013**, *147*, 17–22. [CrossRef] [PubMed]
20. Chan, M.T.; Selvam, A.; Wong, J.W.C. Reducing nitrogen loss and salinity during 'struvite' food waste composting by zeolite amendment. *Bioresour. Technol.* **2016**, *200*, 838–844. [CrossRef] [PubMed]
21. Ministry of Environment (MOE). *A Study on FoodWaste Reduction Equipment Guidelines and Quality Standard P*; Ministry of Environment: Sejong City, Korea, 2009.
22. Yang, X.; Wang, H.; Strong, P.J.; Xu, S.; Liu, S.; Lu, K.; Sheng, K.; Guo, J.; Che, L.; He, L.; et al. Thermal Properties of Biochars Derived from Waste Biomass Generated by Agricultural and Forestry Sectors. *Energies* **2017**, *10*, 469. [CrossRef]
23. Quyn, D.M.; Wu, H.; Li, C.-Z. Volatilisation and catalytic effects of alkali and alkaline earth metallic species during the pyrolysis and gasification of Victorian brown coal. Part I. Volatilisation of Na and Cl from a set of NaCl-loaded samples. *Fuel* **2002**, *81*, 143–149. [CrossRef]
24. Korea Rural Development Administration, National Academy of Agricultural Science. *A Method of Inspection of Physical and Chemical Fertilizers*; Rural Development Administration: Jeonju-si, Korea, 2016.

25. Korea Rural Development Administration, National Academy of Agricultural Science. *Methods of Soil Chemical Analysis*; Rural Development Administration: Jeonju-si, Korea, 2010.
26. Zambon, I.; Colosimo, F.; Monarca, D.; Cecchini, M.; Gallucci, F.; Proto, A.R.; Lord, R.; Colantoni, A. An innovative agro-forestry supply chain for residual biomass: Physicochemical characterisation of biochar from olive and hazelnut pellets. *Energies* **2016**, *9*, 526. [CrossRef]
27. Spokas, K.A. Review of the stability of biochar in soils: Predictability of O:C molar ratios. *Carbon Manag.* **2010**, *1*, 289–303. [CrossRef]
28. Mukome, F.N.D.; Zhang, X.; Silva, L.C.R.; Six, J.; Parikh, S.J. Use of chemical and physical characteristics to investigate trends in biochar feedstocks. *J. Agric. Food Chem.* **2013**, *61*, 2196–2204. [CrossRef] [PubMed]
29. Mukome, F.N.D.; Parikh, S.J. Chemical, Physical, and Surface characterization of Biochar. In *Biochar: Production, Characterization, and Applications*; CRC Press: Boca Raton, FL, USA, 2015.
30. Ok, Y.S.; Uchimiya, S.M.; Chang, S.X.; Bolan, N. (Eds.) *Biochar: Production, Characterization, and Applications*; CRC Press: Boca Raton, FL, USA, 2015.
31. Yuan, J.-H.; Xu, R.-K.; Zhang, H. The forms of alkalis in the biochar produced from crop residues at different temperatures. *Bioresour. Technol.* **2011**, *102*, 3488–3497. [CrossRef] [PubMed]
32. Wu, W.; Yang, M.; Feng, Q.; McGrouther, K.; Wang, H.; Lu, H.; Chen, Y. Chemical characterization of rice straw-derived biochar for soil amendment. *Biomass Bioenergy* **2012**, *47*, 268–276. [CrossRef]
33. Sohi, S.P.; Krull, E.; Lopez-Capel, E.; Bol, R. A review of biochar and its use and function in soil. *Adv. Agron.* **2010**, *105*, 47–82.
34. Zhao, S.-X.; Ta, N.; Wang, X.-D. Effect of Temperature on the Structural and Physicochemical Properties of Biochar with Apple Tree Branches as Feedstock Material. *Energies* **2017**, *10*, 1293. [CrossRef]
35. Van Zwieten, L.; Kimber, S.; Morris, S.; Chan, K.Y.; Downie, A.; Rust, J.; Joseph, S.; Cowie, A. Effects of biochar from slow pyrolysis of papermill waste on agronomic performance and soil fertility. *Plant Soil* **2010**, *327*, 235–246. [CrossRef]
36. Ketterings, Q.; Reid, S.; Rao, R. *Cornell University Agronomy Fact Sheet #22: Cation Exchange Capacity (CEC)*; Cornell University: Ithaca, NY, USA, 2007.
37. Bourke, J.; Manley-Harris, M.; Fushimi, C.; Dowaki, K.; Nunoura, T.; Antal, M.J., Jr. Do all carbonized charcoals have the same chemical structure? 2. A model of the chemical structure of carbonized charcoal. *Ind. Eng. Chem. Res.* **2007**, *46*, 5954–5967. [CrossRef]
38. Guerrero, M.; Ruiz, M.P.; Millera, Á.; Alzueta, M.U.; Bilbao, R. Characterization of biomass chars formed under different devolatilization conditions: Differences between rice husk and eucalyptus. *Energy Fuels* **2008**, *22*, 1275–1284. [CrossRef]
39. Keiluweit, M.; Nico, P.S.; Johnson, M.G.; Kleber, M. Dynamic molecular structure of plant biomass-derived black carbon (biochar). *Environ. Sci. Technol.* **2010**, *44*, 1247–1253. [CrossRef] [PubMed]
40. Herbert, L.; Hosek, I.; Kripalani, R. *The Characterization and Comparison of Biochar Produced from a Decentralized Reactor Using Forced Air and Natural Draft Pyrolysis*; California Polytechnic State University: San Luis Obispo, CA, USA, 2012.
41. Cheng, C.-H.; Lehmann, J.; Thies, J.E.; Burton, S.D.; Engelhardb, M.H. Oxidation of black carbon by biotic and abiotic processes. *Org. Geochem.* **2006**, *37*, 1477–1488. [CrossRef]
42. Boeriu, C.G.; Bravo, D.; Gosselink, R.J.A.; van Dam, J.E.G. Characterisation of structure-dependent functional properties of lignin with infrared spectroscopy. *Ind. Crop. Prod.* **2004**, *20*, 205–218. [CrossRef]
43. Kačuráková, M.; Wilson, R.H. Developments in mid-infrared FT-IR spectroscopy of selected carbohydrates. *Carbohydr. Polym.* **2001**, *44*, 291–303. [CrossRef]
44. Lammers, K.; Arbuckle-Keil, G.; Dighton, J. FT-IR study of the changes in carbohydrate chemistry of three New Jersey pine barrens leaf litters during simulated control burning. *Soil Biol. Biochem.* **2009**, *41*, 340–347. [CrossRef]
45. Kubo, S.; Kadla, J.F. Hydrogen bonding in lignin: A Fourier transform infrared model compound study. *Biomacromolecules* **2005**, *6*, 2815–2821. [CrossRef] [PubMed]
46. Parimala, K.; Balachandran, V. Structural study, NCA, FT-IR, FT-Raman spectral investigations, NBO analysis and thermodynamic properties of 2′, 4′-difluoroacetophenone by HF and DFT calculations. *Spectrochim. Acta Part A Mol. Biomol. Spectrosc.* **2013**, *110*, 269–284. [CrossRef] [PubMed]

47. Porchelvi, E.E.; Muthu, S. The spectroscopic (FT-IR, FT-Raman and NMR), NCA, Fukui function analysis first order hyperpolarizability, TGA of 6-chloro-3, 4dihydro-2H-1, 2, 4-benzothiazine-7-sulphonamide1, 1-dioxide by ab initio HF and Density Functional method. *Spectrochim. Acta Part A Mol. Biomol. Spectrosc.* **2014**, *123*, 230–240. [CrossRef] [PubMed]
48. Mcbeath, A.V.; Smernik, R.J.; Krull, E.S.; Lehmann, J. The influence of feedstock and production temperature on biochar carbon chemistry: A solid-state 13 C NMR study. *Biomass Bioenergy* **2014**, *60*, 121–129. [CrossRef]
49. Knicker, H.; Hilscher, A.; González-Vila, F.J.; Almendros, G. A new conceptual model for the structural properties of char produced during vegetation fires. *Org. Geochem.* **2008**, *39*, 935–939. [CrossRef]
50. Brewer, C.E.; Unger, R.; Schmidt-Rohr, K.; Brown, R.C. Criteria to select biochars for field studies based on biochar chemical properties. *BioEnergy Res.* **2011**, *4*, 312–323. [CrossRef]